Cell, Volume *138*

Supplemental Data

Androgen Receptor Regulates a Distinct Transcription Program in Androgen-Independent Prostate Cancer

Qianben Wang, Wei Li, Yong Zhang, Xin Yuan, Kexin Xu, Jindan Yu, Zhong Chen, Rameen Beroukhim, Hongyun Wang, Mathieu Lupien, Tao Wu, Meredith M. Regan, Clifford A. Meyer, Jason S. Carroll, Arjun Kumar Manrai, Olli A. Jänne, Steven P. Balk, Rohit Mehra, Bo Han, Arul M. Chinnaiyan, Mark A. Rubin, Lawrence True, Michelangelo Fiorentino, Christopher Fiore, Massimo Loda, Philip W. Kantoff, X. Shirley Liu, and Myles Brown

Figure S1. Molecular basis for androgen-independent faster growth of AIPC. (A) abl cells grow faster than LNCaP cells in the absence of androgen. The cell proliferation was measured using the WST-1 assay on day 0, day 2 and day 4 in the absence or presence of DHT from 0.01 nM to 100 nM. (B) Summary of differentially expressed genes ($q<0.05$) from abl/LNCaP gene expression profile and two clinical AIPC/ADPC datasets. Red segments represents up-regulated genes, and green segments represents down-regulated genes.

A

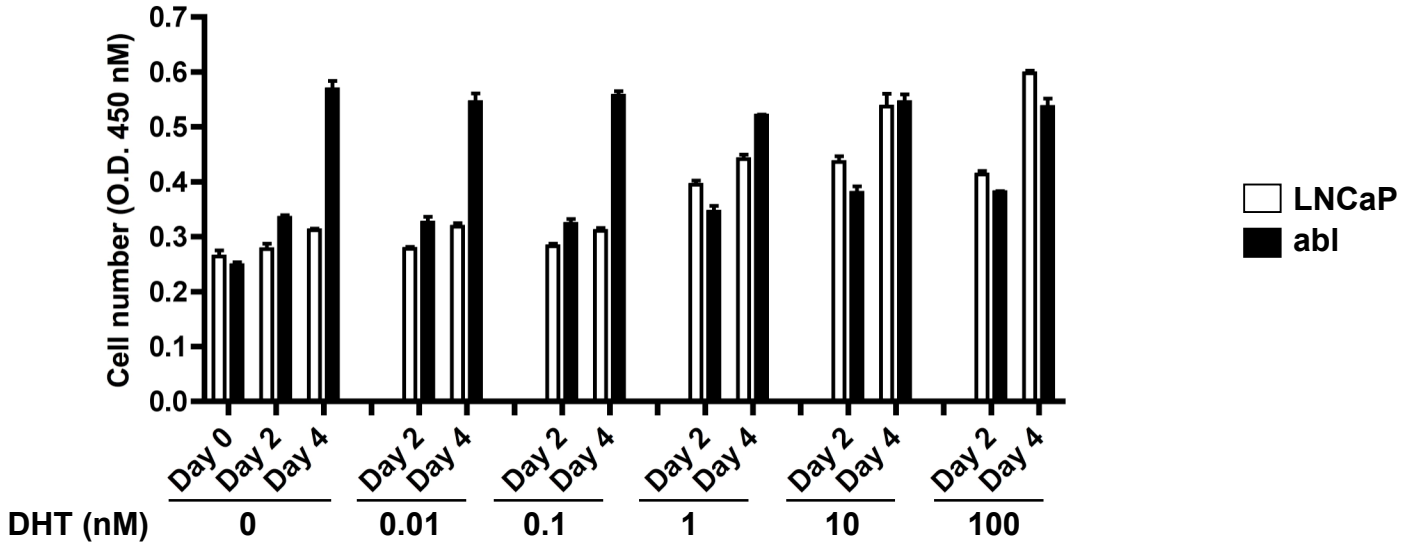
Cell number (O.D. 450 nM)
0.7
0.6
0.5
0.4
0.3
0.2
0.1
0.0
Day 0
Day 2
Day 4
DHT (nM)
0
0.01
0.1
1
10
100
LNCaP
abl

B

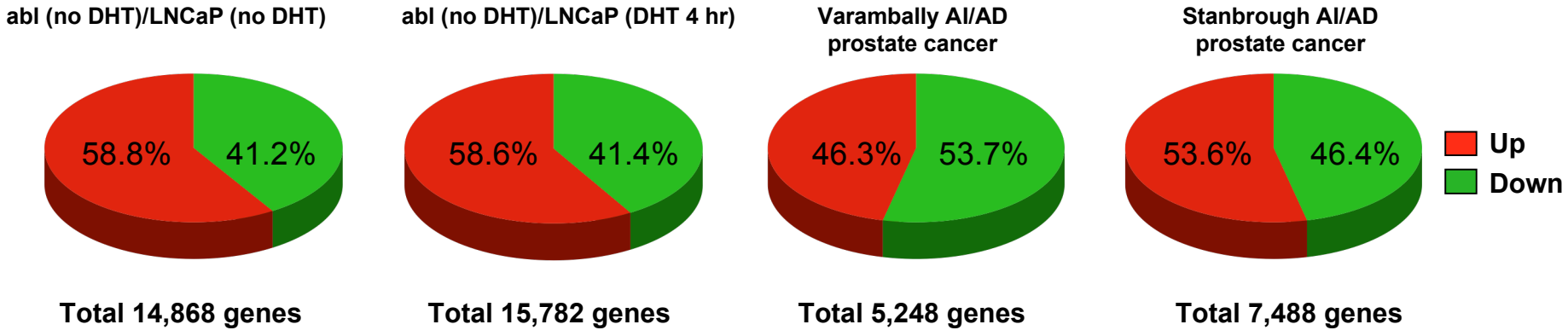
abl (no DHT)/LNCaP (no DHT)
58.8%
41.2%
Total 14,868 genes
abl (no DHT)/LNCaP (DHT 4 hr)
58.6%
41.4%
Total 15,782 genes
Varambally AI/AD prostate cancer
46.3%
53.7%
Total 5,248 genes
Stanbrough AI/AD prostate cancer
53.6%
46.4%
Total 7,488 genes
Up
Down

Figure S2. Independent AR siRNAs have same effects on decreasing abl basal AR up-regulated genes. abl cells were transfected with two independent AR siRNAs as described in Figure 1A. Seventy-two hr after siRNA transfection, real-time RT-PCR was performed using transcript-specific primers (Table S1).

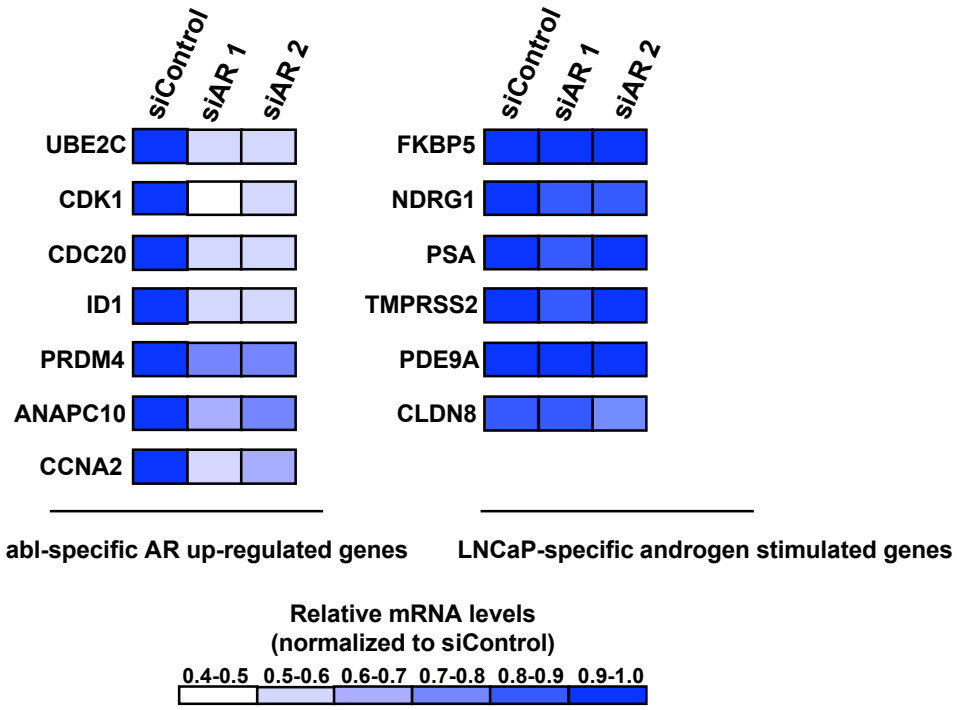
siControl
siAR 1
siAR 2
UBE2C
CDK1
CDC20
ID1
PRDM4
ANAPC10
CCNA2
siControl
siAR 1
siAR 2
FKBP5
NDRG1
PSA
TMPRSS2
PDE9A
CLDN8
abl-specific AR up-regulated genes
LNCaP-specific androgen stimulated genes
Relative mRNA levels
(normalized to siControl)
0.4-0.5
0.5-0.6
0.6-0.7
0.7-0.8
0.8-0.9
0.9-1.0

Figure S3. Map of whole genome AR binding in LNCaP and abl cells. Red and dark color represents AR binding in LNCaP and abl cells, respectively.

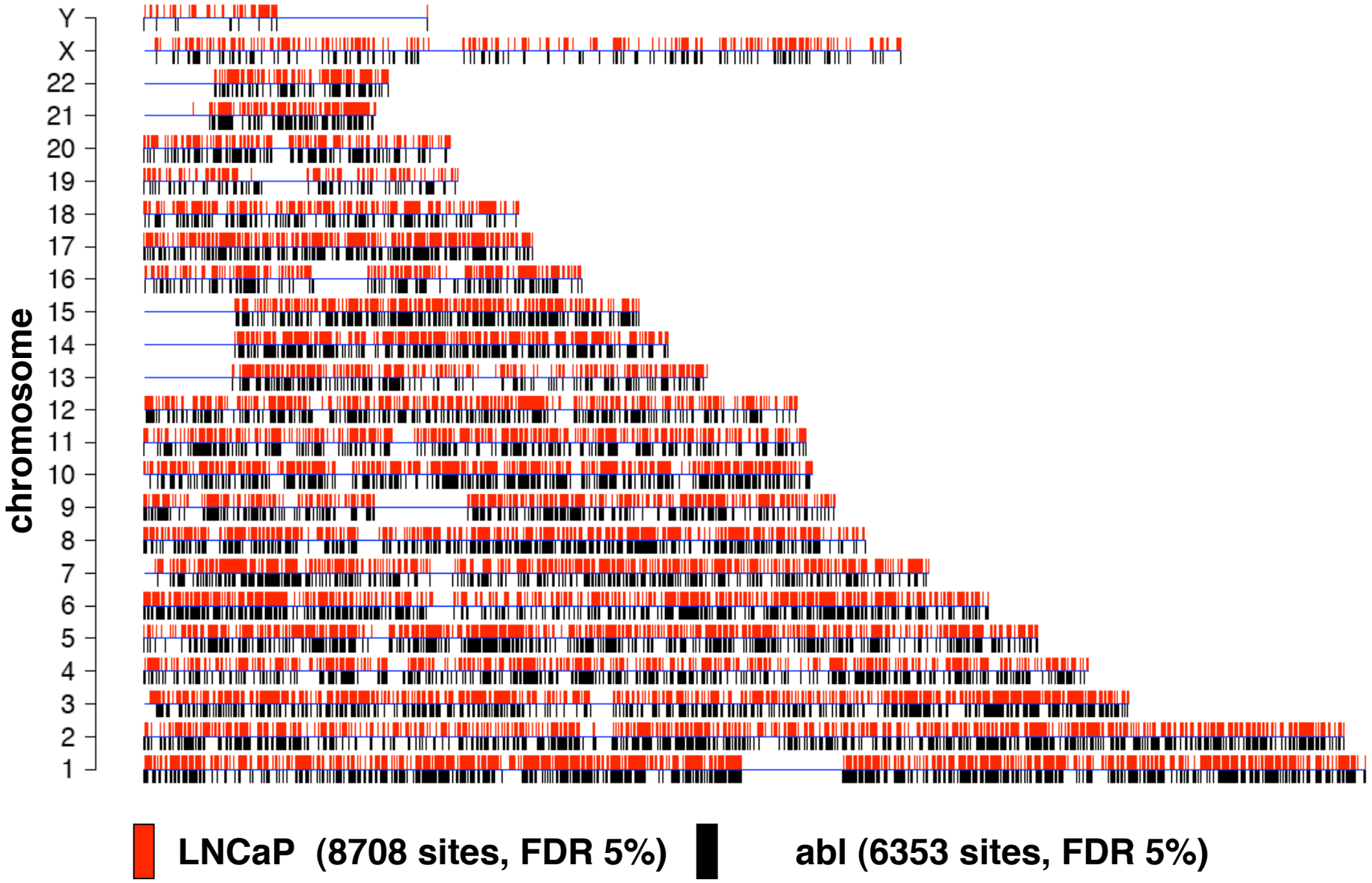
chromosome
Y
X
22
21
20
19
18
17
16
15
14
13
12
11
10
9
8
7
6
5
4
3
2
1
LNCaP (8708 sites, FDR 5%)
abl (6353 sites, FDR 5%)

Figure S4. Quality controls for ChIP-on-chip binding data. Bar files were generated after MAT analysis of AR whole genome ChIP-on-chip raw data from LNCaP and abl cells. AR binding peaks at the KLK3 (PSA) enhancer (Schuur et al., 1996), the KLK2 promoter and enhancer (Sun et al., 1997; Yu et al., 1999), and the TMPRSS2 enhancer (Wang et al., 2007) were indicated by arrows.

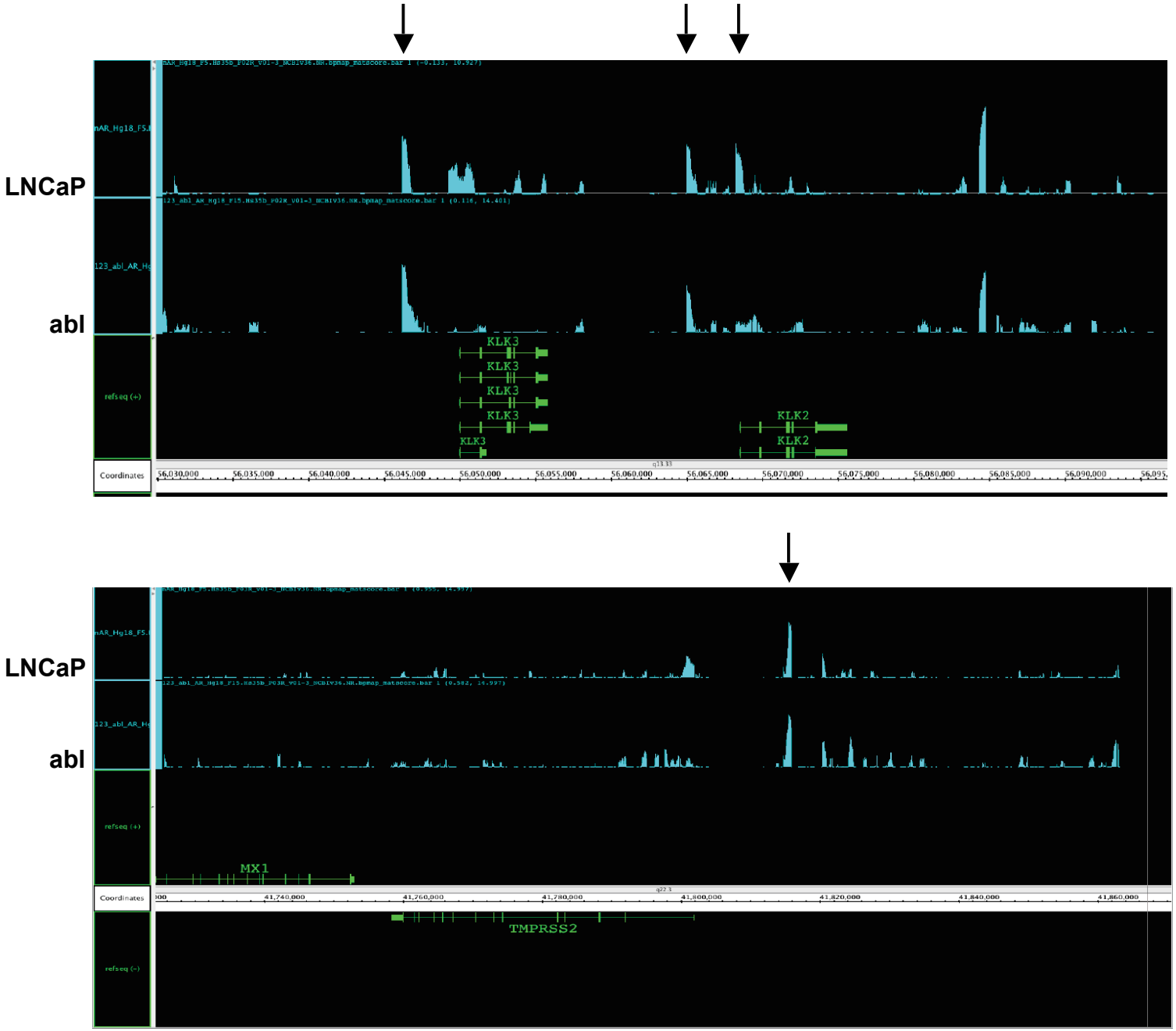
LNCaP
abl
KLK3
KLK3
KLK3
KLK3
KLK3
KLK2
KLK2
refseq (+)
Coordinates
LNCaP
abl
MX1
TMPRSS2
refseq (+)
refseq (-)
Coordinates

Figure S5. Comparison of AR binding in LNCaP and abl cells. The pseudo fold-change of the same AR binding site between two cell lines were determined from the scoring formula, Fold_Change = (MS1 – MS2) / maximum (MS_cutoff, minimum (MS1, MS2)). Where MS1 and MS2 are MAT scores of the same AR binding site in two cell lines, MS_cutoff is the corresponding MAT score (around 3.7) for the 1×10^{-4} p value cutoff. The differential AR binding sites (3,716 sites in abl cells and 6,592 sites in LNCaP cells) have fold change ≤0.5 or ≥2. The other AR bindings have same binding affinity in two cell lines (5,424 sites).

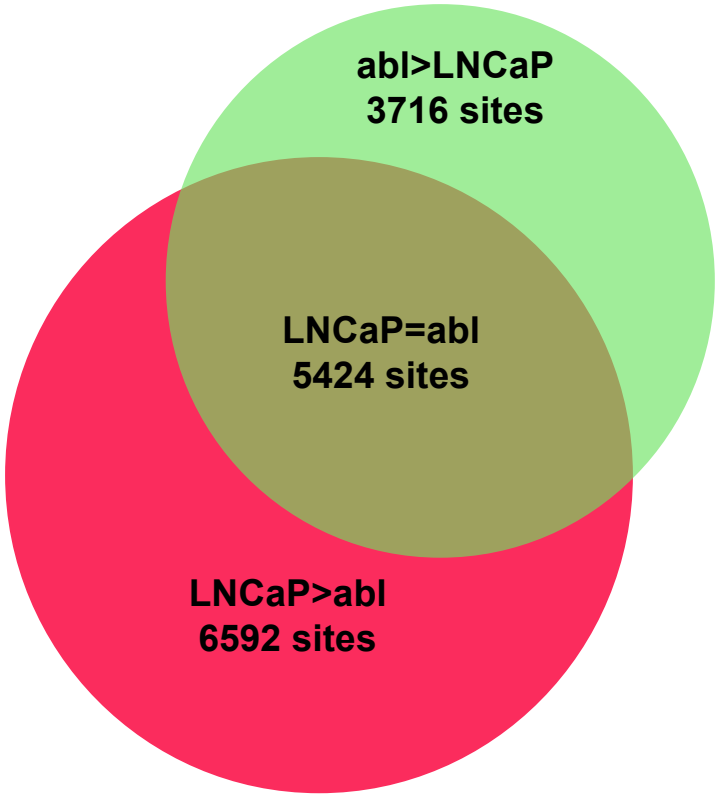
abl>LNCaP
3716 sites
LNCaP=abl
5424 sites
LNCaP>abl
6592 sites

Figure S6. Effects of distance on AR binding enrichment near differentially expressed genes. The percentages for each category of genes that have a AR binding site were calculated with distance from 10 kb to 100 kb (10 kb as interval), and then the percentages were divided by the corresponding percentages for control category to derive the enrichment folds in LNCaP cells (A) and abl cells (B).

A

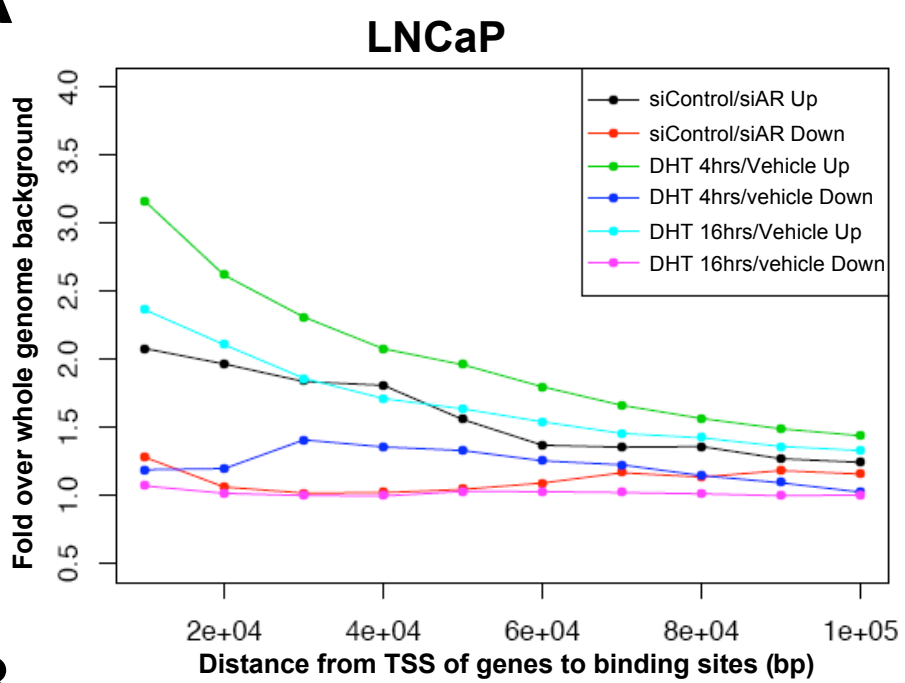
LNCaP
Fold over whole genome background
0.5
1.0
1.5
2.0
2.5
3.0
3.5
4.0
2e+04
4e+04
6e+04
8e+04
1e+05
Distance from TSS of genes to binding sites (bp)
siControl/siAR Up
siControl/siAR Down
DHT 4hrs/Vehicle Up
DHT 4hrs/vehicle Down
DHT 16hrs/Vehicle Up
DHT 16hrs/vehicle Down

B

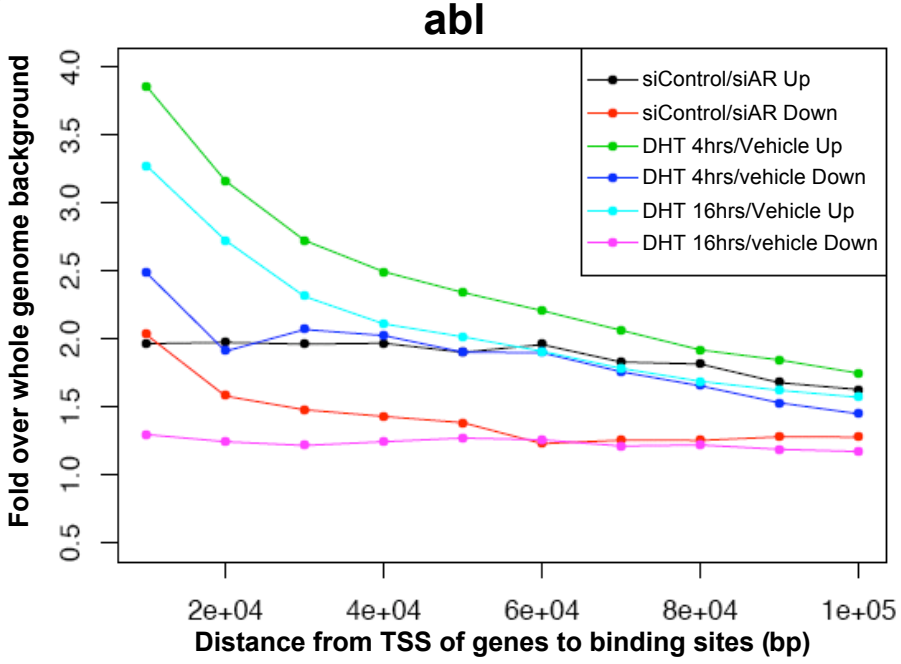
abl
Fold over whole genome background
0.5
1.0
1.5
2.0
2.5
3.0
3.5
4.0
2e+04
4e+04
6e+04
8e+04
1e+05
Distance from TSS of genes to binding sites (bp)
siControl/siAR Up
siControl/siAR Down
DHT 4hrs/Vehicle Up
DHT 4hrs/vehicle Down
DHT 16hrs/Vehicle Up
DHT 16hrs/vehicle Down

Figure S7. AR binding sites in abl cells relative to the *UBE2C* gene shown using the UCSC genome browser format.

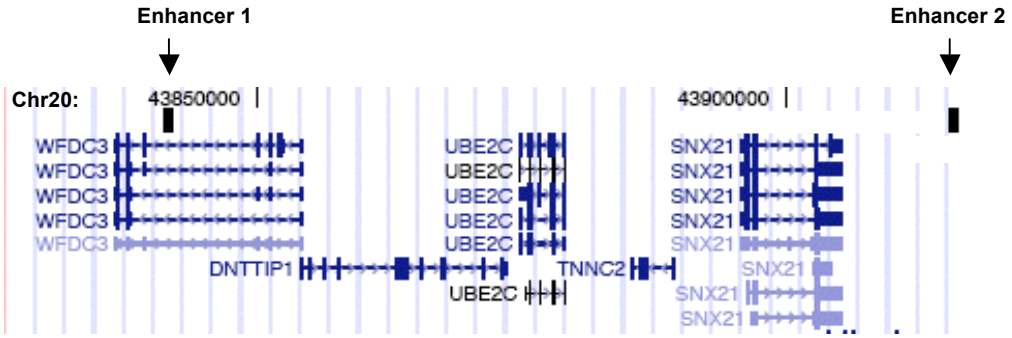
Enhancer 1
Enhancer 2
Chr20:
43850000
43900000
WFDC3
WFDC3
WFDC3
WFDC3
WFDC3
DNTTIP1
UBE2C
UBE2C
UBE2C
UBE2C
UBE2C
UBE2C
TNNC2
SNX21
SNX21
SNX21
SNX21
SNX21
SNX21
SNX21
SNX21

Figure S8. KDM1 over-expression decreases H3K4me2 and FoxA1 levels at the UBE2C enhancers in LNCaP and abl cells. LNCaP and abl cells were transfected with pCMX-FLAG-KDM1 or pCMX-FLAG vector. Three days after transfection, cells treated with (+) or without (-) DHT for 4 hr. H3K4me2 and FoxA1ChIP were then performed.

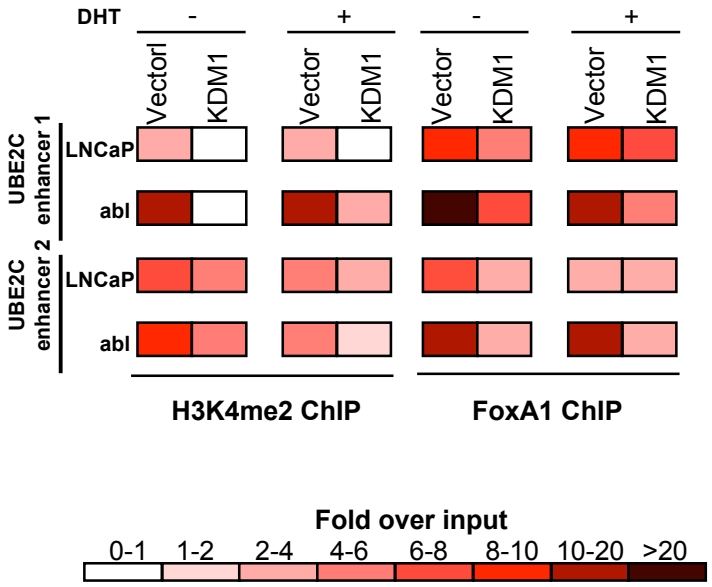
DHT
-
+
-
+
Vector
KDM1
Vector
KDM1
Vector
KDM1
Vector
KDM1
UBE2C enhancer 1
LNCaP
abl
UBE2C enhancer 2
LNCaP
abl
H3K4me2 ChIP
FoxA1 ChIP
Fold over input
0-1
1-2
2-4
4-6
6-8
8-10
10-20
>20

Figure S9. FoxA1 silencing does not affect differential H3K4me2 level on the UBE2C enhancers. LNCaP and abl cells were transfected with siFoxA1 or siControl. Three days after transfection, cells treated with (+) or without (-) DHT for 4 hr. H3K4me2 ChIP was then performed.

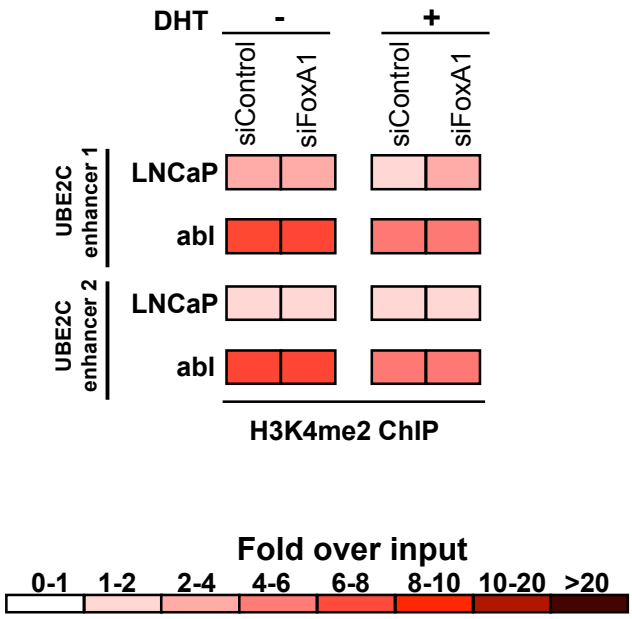
DHT
-
+
siControl
siFoxA1
siControl
siFoxA1
UBE2C enhancer 1
LNCaP
abl
UBE2C enhancer 2
LNCaP
abl
H3K4me2 ChIP
Fold over input
0-1
1-2
2-4
4-6
6-8
8-10
10-20
>20

Figure S10. H3K4me1, H3K4me2 and FoxA1 are specifically present on AR binding regions near cell cycle genes. Levels of H3K4me1 and H3K4me2 (A), and FoxA1 (B) on UBE2C enhancer 2 (positive control), CDK1 enhancer, CDC20 enhancer, ANAPC10 enhancer and 7 randomly selected AREs that do not have AR binding were determined by ChIP assays in the absence (-) and presence (+) of DHT. (mean (n=2) ± s.e.).

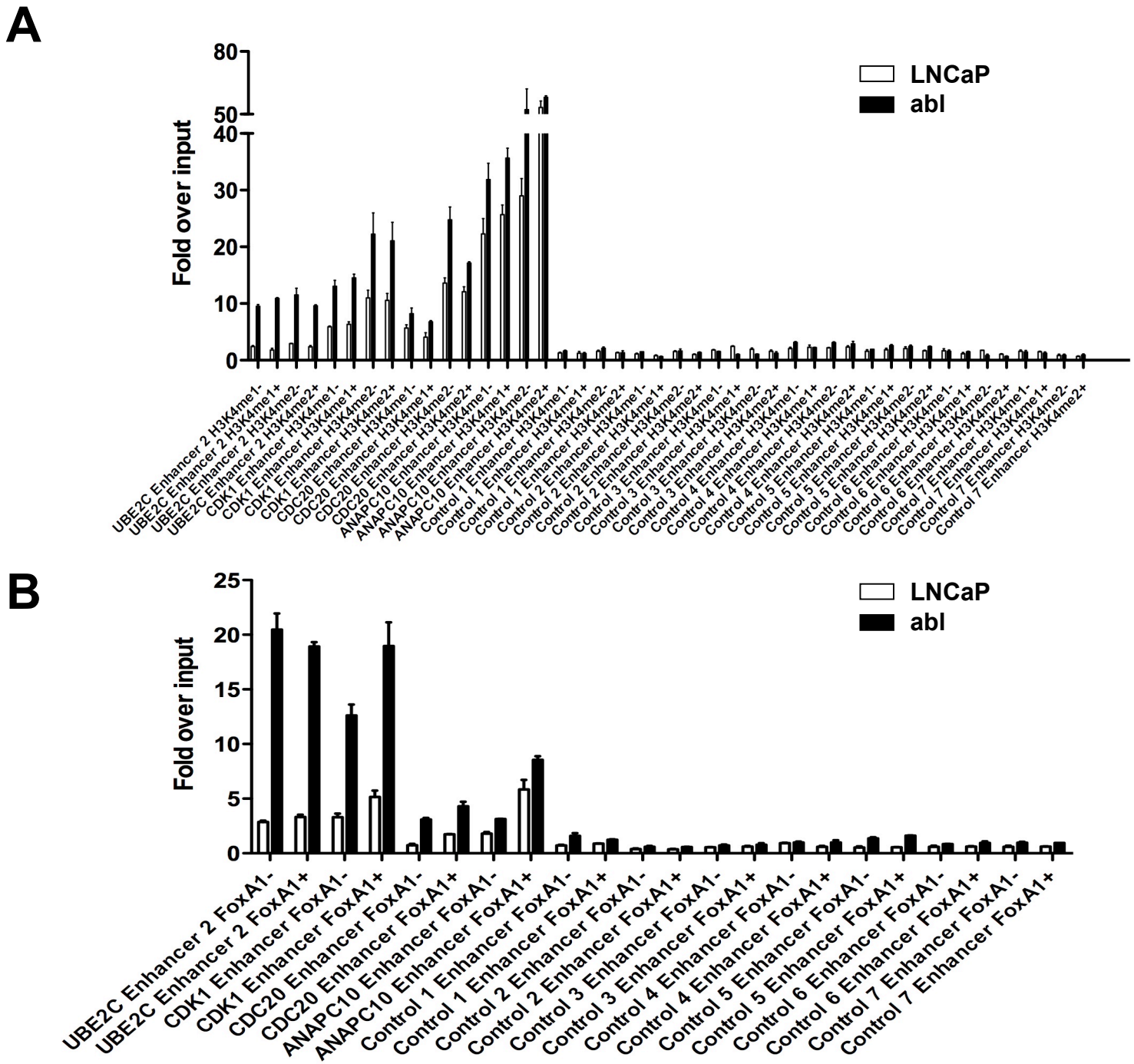
A
Fold over input
LNCaP
abl
B
Fold over input
LNCaP
abl
UBE2C Enhancer 2 FoxA1-
UBE2C Enhancer 2 FoxA1+
CDK1 Enhancer FoxA1-
CDK1 Enhancer FoxA1+
CDC20 Enhancer FoxA1-
CDC20 Enhancer FoxA1+
ANAPC10 Enhancer FoxA1-
ANAPC10 Enhancer FoxA1+
Control 1 Enhancer FoxA1-
Control 1 Enhancer FoxA1+
Control 2 Enhancer FoxA1-
Control 2 Enhancer FoxA1+
Control 3 Enhancer FoxA1-
Control 3 Enhancer FoxA1+
Control 4 Enhancer FoxA1-
Control 4 Enhancer FoxA1+
Control 5 Enhancer FoxA1-
Control 5 Enhancer FoxA1+
Control 6 Enhancer FoxA1-
Control 6 Enhancer FoxA1+
Control 7 Enhancer FoxA1-
Control 7 Enhancer FoxA1+

Figure S11. Over-expression of KDM1 (A) and silencing of FoxA1 (B) significantly decrease AR binding at the CDK1 and CDC20 enhancers. The experiments were performed as in Figure 5 except that AR ChIPs were performed on the CDK1 and CDC20 enhancer.

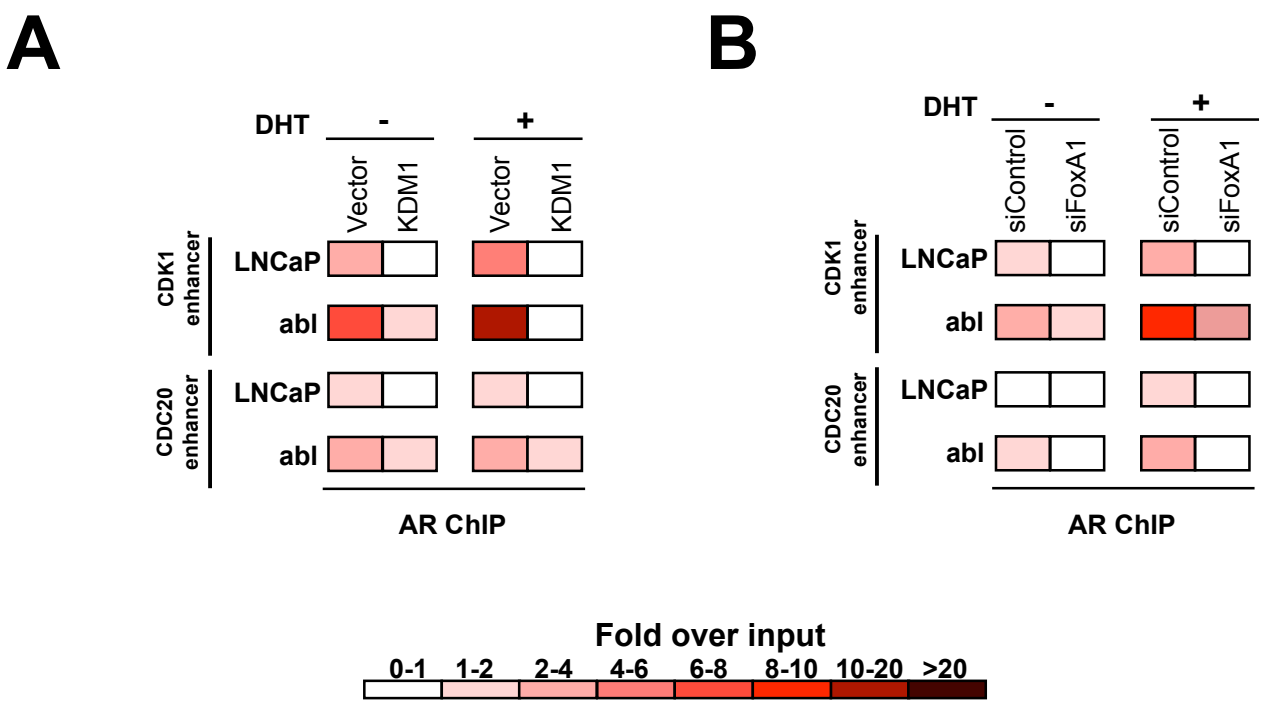
A
DHT
-
+
Vector
KDM1
Vector
KDM1
CDK1 enhancer
LNCaP
abl
CDC20 enhancer
LNCaP
abl
AR ChIP
B
DHT
-
+
siControl
siFoxA1
siControl
siFoxA1
CDK1 enhancer
LNCaP
abl
CDC20 enhancer
LNCaP
abl
AR ChIP
Fold over input
0-1
1-2
2-4
4-6
6-8
8-10
10-20
>20

Figure S12. Over-expression of UBE2C does not increase AR binding at the M-phase gene enhancers in LNCaP cells. LNCaP cells were transfected with UBE2C or a UBE2C mutant (C114S). Three days later cells were treated with DHT or vehicle for 4 hr and AR ChIP assays were performed on the CDC20, CDK1 and ANAPC10 enhancers. abl cells without transfection was used as controls.

A

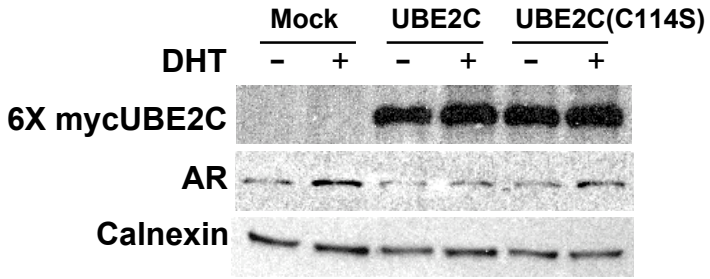
Mock
UBE2C
UBE2C(C114S)
DHT
– + – + – +
6X mycUBE2C
AR
Calnexin

B

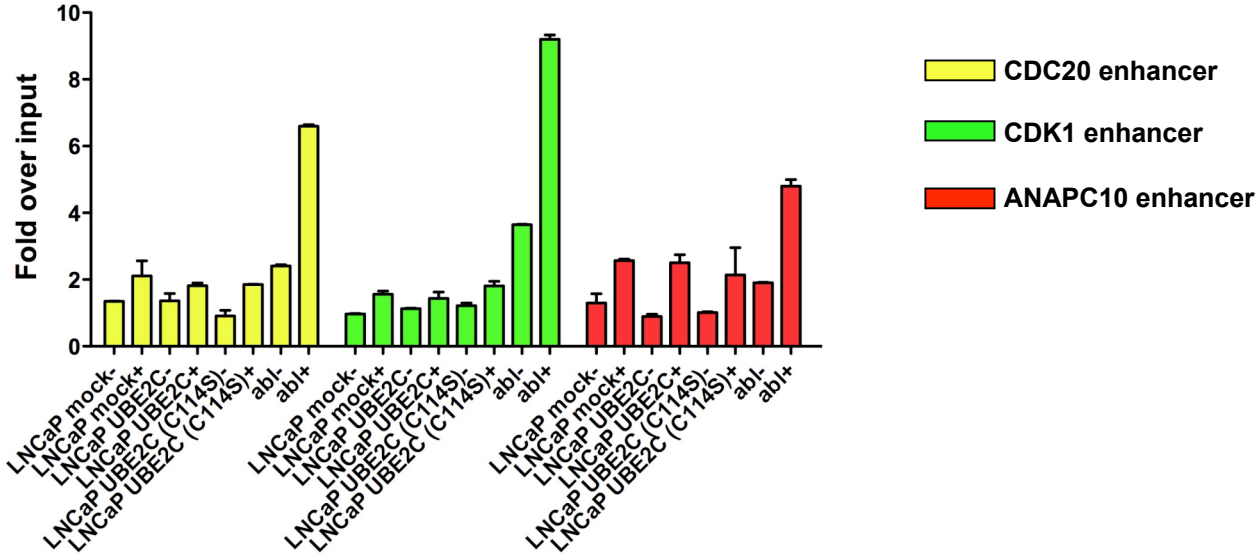
Fold over input
10
8
6
4
2
0
LNCaP mock-
LNCaP mock+
LNCaP UBE2C-
LNCaP UBE2C+
LNCaP UBE2C (C114S)-
LNCaP UBE2C (C114S)+
abl-
abl+
CDC20 enhancer
CDK1 enhancer
ANAPC10 enhancer

Figure S13. AR-regulated high UBE2C protein expression level in androgen-independent cell line C4-2B. Western blots were performed using the antibodies indicated ninety-six hrs after siRNA transfection.

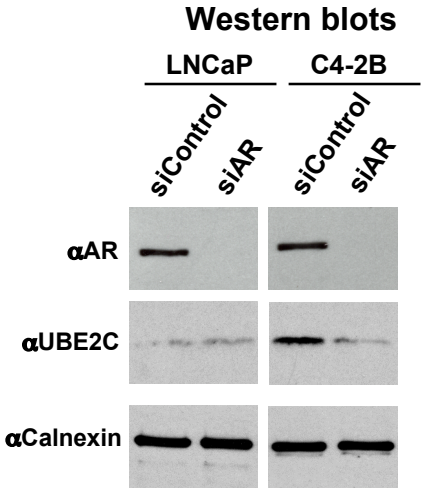
Western blots
LNCaP
C4-2B
siControl
siAR
siControl
siAR
αAR
αUBE2C
αCalnexin

Figure S14. Greater H3K4 methylation, FoxA1 recruitment and AR binding on the UBE2C enhancers in a clinical case of AIPC than in an ADPC case. ChIP was performed using tissues from one ADPC and one AIPC (mean (n=2) ±s.e.). Tissue ChIP was performed using standard ChIP protocols as previously described (Yu et al., 2007) with the following modifications. Primary tissues were chopped into small pieces with a razor blade and transferred into 5-10 ml of PBS for crosslinking in 1% formaldehyde for 15 minutes. The crosslinking was stopped by 1/20V of 2.5M Glycine and the cells were washed with 1xPBS and harvested in 1xPBS with protease inhibitors. The tissue pellets were further disaggregated using a tissue homogenizer. The cells were then pelleted and resuspended in cell lysis buffer containing protease inhibitors for 10 min. The samples were then resuspended in nuclei lysis buffer for 10-20 min. Prior to sonication 0.1g of glass beads were added to the lysate and DNA were sonicated to an average size of 400bp.

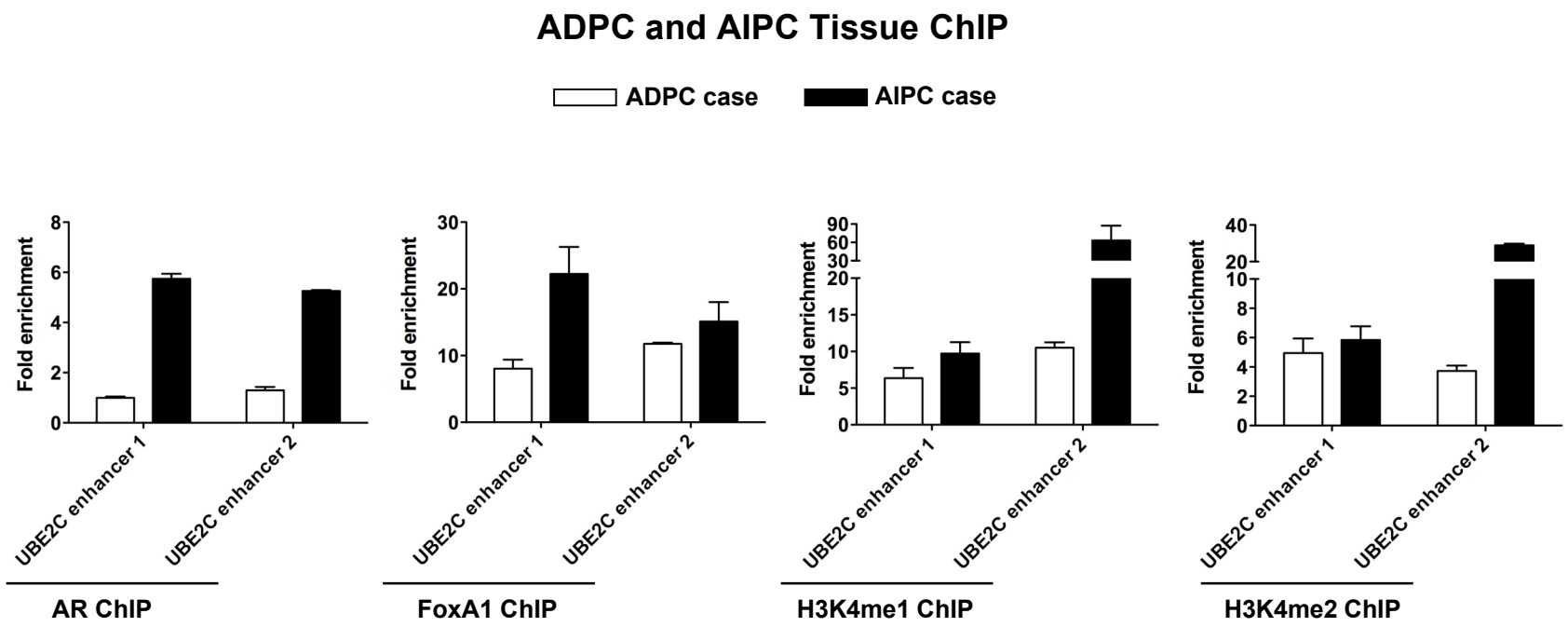
ADPC and AIPC Tissue ChIP
ADPC case
AIPC case
Fold enrichment
UBE2C enhancer 1
UBE2C enhancer 2
AR ChIP
FoxA1 ChIP
H3K4me1 ChIP
H3K4me2 ChIP

Figure S15. Over-expression of UBE2C in LNCaP cells cannot accelerate their proliferation in the absence of androgen. LNCaP cells were grown in phenol-red free RPMI 1640 supplemented with 10% FBS. Cells were transfected with a wild-type UBE2C construct or a catalytically dead active-site mutant (C114S) (Reddy et al., 2007) using Lipofectamine 2000. Western blot (A) was performed to confirm over-expression of UBE2C proteins. The cell proliferation was measured on day 2 and day 4 after transfection using the WST-1 assay (mean (n=3) ± s.e.).

A

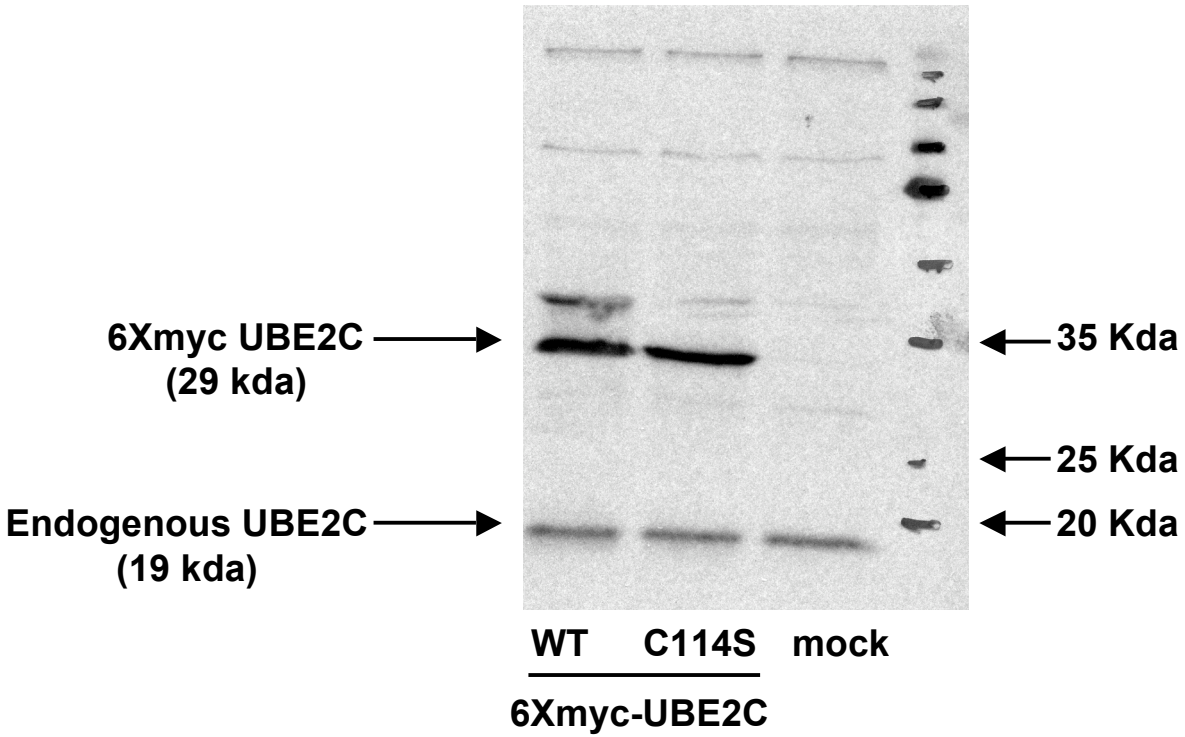
6Xmyc UBE2C
(29 kda)
Endogenous UBE2C
(19 kda)
35 Kda
25 Kda
20 Kda
WT
C114S
mock
6Xmyc-UBE2C

B

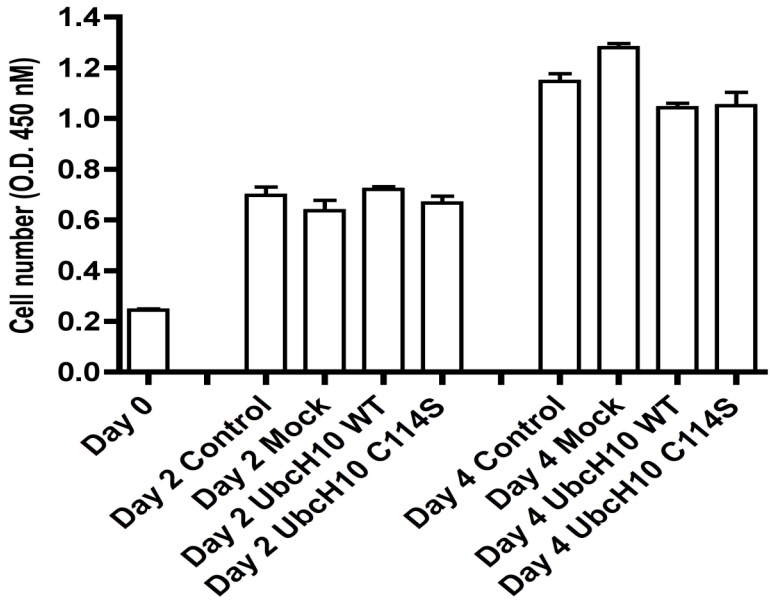
Cell number (O.D. 450 nM)
1.4
1.2
1.0
0.8
0.6
0.4
0.2
0.0
Day 0
Day 2 Control
Day 2 Mock
Day 2 UbcH10 WT
Day 2 UbcH10 C114S
Day 4 Control
Day 4 Mock
Day 4 UbcH10 WT
Day 4 UbcH10 C114S

Figure S16. UBE2C protein has same half-life in LNCaP and abl cells. LNCaP and abl cells were treated with 0.1mg/ml cycloheximide (CHX). Cells were collected at indicated time points, and subjected to immunoblotting. The band intensities in LNCaP and abl cells were quantified using FluorChem5500 and normalized to their own time 0.

A

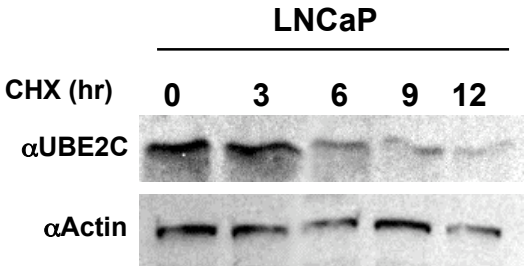
LNCaP
CHX (hr)
0
3
6
9
12
αUBE2C
αActin

B

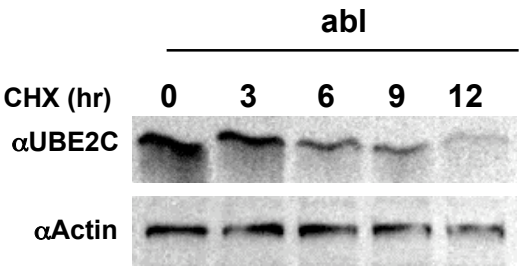
abl
CHX (hr)
0
3
6
9
12
αUBE2C
αActin

C

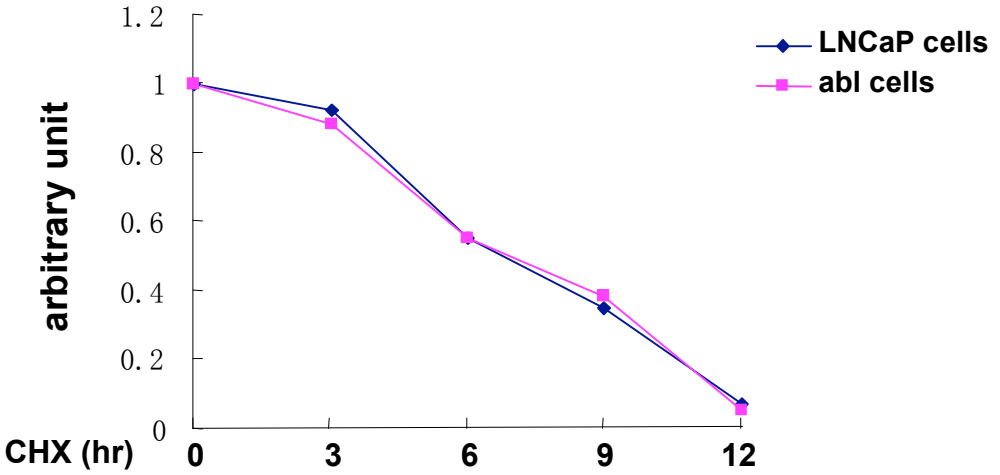
1.2
1
0.8
0.6
0.4
0.2
0
arbitrary unit
CHX (hr)
0
3
6
9
12
LNCaP cells
abl cells

Figure S17. The effects of CDK1 and CDC20 silencing on LNCaP and abl cell proliferation. siRNA-WST1 experiments were performed as in Figure 7A.

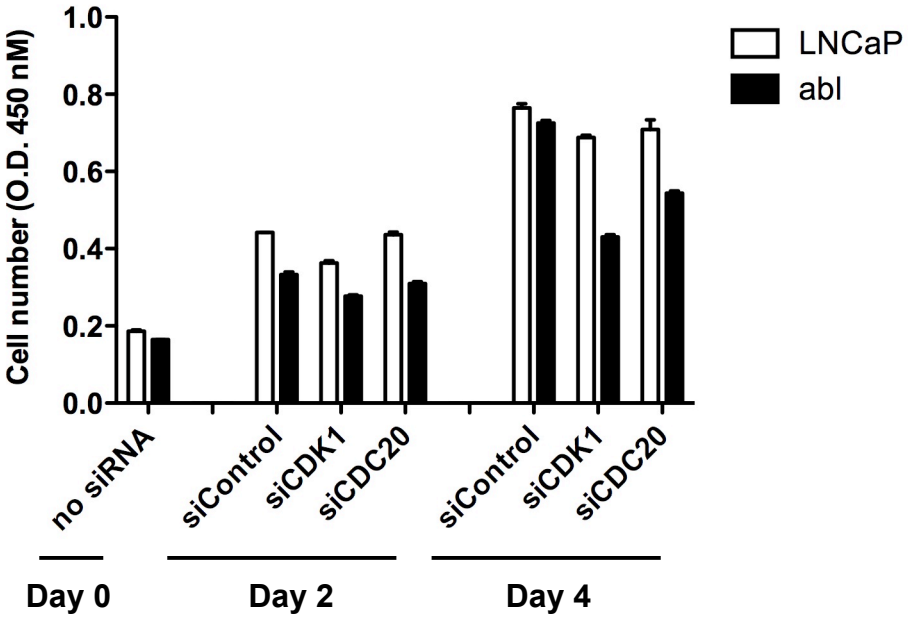
Cell number (O.D. 450 nM)
1.0
0.8
0.6
0.4
0.2
0.0
LNCaP
abl
no siRNA
siControl
siCDK1
siCDC20
siControl
siCDK1
siCDC20
Day 0
Day 2
Day 4

Table S1

ChIP and 3C primers	Sequences
CDC20 enhancer+	GGAGTTGTGAGAACACCCGG
CDC20 enhancer-	AACACCCAGGTACACCCTCG
CDK1 enhancer+	GGGAAAGAGAAGCCCTACACTTG
CDK1 enhancer-	GGGCTGTGCTACTTCTCTGGG
UBE2C enhancer 1+	TGCCTCTGAGTAGGAACAGGTAAGT
UBE2C enhancer 1-	TGCTTTTTCCATCATGGCAG
UBE2C enhancer 2+	CCACAAACTCTTCTCAGCTGGG
UBE2C enhancer 2-	TTCTTTCCTTCCCTGTTACCCC
UBE2C promoter+	TGCCCGAGGGAAATTGG
UBE2C promoter-	CTTACTCCGCGTGGGAACA
ANAPC10 enhancer+	CCAAAGGTATCAAACTGACATCTTTC
ANAPC10 enhancer-	CAAAAATTTCCTGTCCTTCTTTGC
SGOL2 enhancer+	GGGAGACGCTGGAATCTGAG
SGOL2 enhancer-	TGGACGGTTCAGCCTTGAG
PSA promoter+ (Jia et al., 2003)	CCTAGATGAAGTCTCCATGAGCTACA
PSA promoter-(Jia et al., 2003)	GGGAGGGAGAGCTAGCACTTG
PSA enhancer + (Wang et al., 2005)	TGGGACAACTTGCAAACCTG
PSA enhancer- (Wang et al., 2005)	CCAGAGTAGGTCTGTTTTCAATCCA
CCNA2 enhancer+	TTAGTGAGCTGTCCAGTGACTCAAT
CCNA2 enhancer-	CCCATGTATTAAAGTAGCTTCTGTAAACA
BUB3 enhancer+	AGAAATTCGGGTCAAAATATGTTGT
BUB3 enhancer-	TGCAGTTGGTATTGCCAACAG
PRDM4 enhancer +	CAGCATGAAGCTTGCAGAATTAA
PRDM4 enhancer-	CACCTTGAGTTTTGCTGGTATGG
GNL3 enhancer+	GAGGTGTTGGATGCCAGAGATC
GNL3 enhancer-	CACTCTGGACAATGGCCTCTTC
BTG3 enhancer+	GCCAATTTTTGGCAAATTTACAT
BTG3 enhancer-	CTGCTACTTTGCTTTCATCTTATTAATCTT
BCCIP enhancer+	TGCAGTTTTCCCTTCCTTCTTC
BCCIP enhancer-	CAAAGATTTACCCACGACTTGGT
CDKN3 enhancer+	AGCTACTCACGTGCCAAATGG
CDKN3 enhancer-	GTTCGCGGCCTTCTGCTA
ID1 enhancer +	GCGCCGTCTCCATCCTAA
ID1 enhancer -	GCAGGGTGACGTGACAGTTG
DBF4 enhancer+	TGACGCGTTTTCAAATCTTCA
DBF4 enhancer-	GGAGGAAGGCGCAAAGC
UBE2C enhancer 2+ (tissue ChIP)	ACAAAATGAAGGGGGAAACC
UBE2C enhancer 2- (tissue ChIP)	CTGTTACCCCCAGAGCAGAT
Control ARE region1+	CACAGAATCAGTCTAGGGTGCTCTT

Control ARE region1-	CTGCATGCTCAAGGAGTGTGTT
Control ARE region2+	GCTGATTCAATTACCTCCCAGAA
Control ARE region2-	AGTTTGGGACAGACGGGAAA
Control ARE region3+	CCCATGCCAGCAGTAGCTAGA
Control ARE region3-	GCACTCACAGAATGCACAGAAAA
Control ARE region4+	AAGAGGGACCATCTCATTTTGG
Control ARE region4-	GCTGTCTCCCCGACCTTTC
Control ARE region5+	CCCTGAAAGAAAAGAGCTGTCAGT
Control ARE region5-	TTTGCAGTGAGTGCTATGAGAAACT
Control ARE region6+	GCCTGGCTGAGTCGGTCAT
Control ARE region6-	GGAGTAAAGCTGCTCAGGGAGAA
Control ARE region7+	GGTTACACACGTTAGGTATTCATCATG
Control ARE region7-	TTGCTGTGCCCGTGTAGCT
3C Taqman probe	6FAMCAGGAGGTGGCGGCMGBNFQ
3C anchor (A)	TAGGCATTGGTACCCAGAGCA
3C control 1 (C1)	GGCTCTCTGACCGACTCCTTCT
3C control 2 (C2)	ATTGCCAGCCAGCCCAG
3C control 3 (C3)	AGGCGTCAGCCACTGTGC
3C enhancer 1 (E1)	TGGCTTGCATGGCAGATTT
3C enhancer 2 (E2)	AGCCATGTTCGTGCCACTG
3C GADPH loading control+(Hagege et al., 2007)	ACAGTCCATGCCATCACTGCC
3C GADPH loading control-(Hagege et al., 2007)	GCCTGCTTCACCACCTTCTTG
3C GADPH Bgl II control+	CCTTCTCCCCATTCCGTCTT
3C GADPH Bgl II control-	TGTGCGGTGTGGGATTGTC

RT-PCR primers

AR mRNA+ (Bieche et al., 2001)	CCTGGCTTCCGCAACTTACAC
AR mRNA-(Bieche et al., 2001)	GGACTTGTGCATGCGGTACTCA
CDC20 mRNA+ (Yuan et al., 2006)	CCTCTGGTCTCCCCATTAC
CDC20 mRNA- (Yuan et al., 2006)	ATGTGTGACCTTTGAGTTCAG
UBE2C mRNA+ (Okamoto et al., 2003)	TGGTCTGCCCTGTATGATGT
UBE2C mRNA- (Okamoto et al., 2003)	AAAAGCTGTGGGGTTTTTCC
CDK1mRNA+	CCTAGTACTGCAATTCGGGAAATT
CDK1 mRNA-	CCTGGAATCCTGCATAAGCAC
PRDM4 mRNA+	CACCTTCACTGCAAATGGAA
PRDM4 mRNA-	AAGTCACTGGTCCATGTTCG
ID1 mRNA+(Lofstedt et al., 2004)	CTACGACATGAACGGCTGTTACTC

ID1 mRNA- (Lofstedt et al., 2004)	CTTGCTCACCTTGCGGTTCT
ANAPC10 mRNA+	CTGATGAAAGCTATACTCCAAGCA
ANAPC10 mRNA-	GGAACATGAATCCAGCCACT
CCNA2 mRNA+	CAGAAAACCATTGGTCCCTC
CCNA2 mRNA-	CACTCACTGGCTTTTCATCTTC
CDKN1A mRNA+	TGCGTTCACAGGTGTTTCTG
CDKN1A mRNA-	GTCCACTGGGCCGAAGAG
BUB3 mRNA+	AATGCTGGGACCTTCTCTCA
BUB3 mRNA-	TCCGTAAGTCCCACACCAA
BCCIP mRNA+	GAAAACCTGAGGTGCTTGGA
BCCIP mRNA-	TCAGAGAAACCAGGGCTGTC
CDKN3 mRNA+	TCATGGCTATCTTTGTCACGA
CDKN3 mRNA-	TCTTTTTGGACATTTCTTCTAACA
BTG3 mRNA+	TGTATAGTGACCTGGGCTTGC
BTG3 mRNA-	TCAAAGCTGGCAACAATGAA
GNL3 mRNA+	TCCTCAGGTAGAAGAGGCCA
GNL3 mRNA-	GCCAGCTCTCCAAATTCTCC
DBF4 mRNA+	ATGGGGAGTAAAAATTCTTCATATTG
DBF4 mRNA-	TGCACCACTACCAACTCTTTTG
PSA mRNA+(Wang et al., 2007)	TGTGTGCTGGACGCTGGA
PSA mRNA-(Wang et al., 2007)	CACTGCCCCATGACGTGAT
TMPRSS2 mRNA+(Wang et al., 2007)	GGACAGTGTGCACCTCAAAGAC
TMPRSS2 mRNA-(Wang et al., 2007)	TCCCACGAGGAAGGTCCC
PDE9A mRNA+(Wang et al., 2007)	GATCCCAATGTTTGAAACAGTGAC
PDE9A mRNA-(Wang et al., 2007)	TCCCAAAGTGGCTGCAGC
CLDN8 mRNA+(Wang et al., 2007)	CGGCTGGAATCATCTTCATCA
CLDN8 mRNA-(Wang et al., 2007)	TTGGCAACCCAGCTCACAG
FKBP5 mRNA+	GCGGAGAGTGACGGAGTC
FKBP5 mRNA-	TGGGGCTTTCTTCATTGTTC
NRDG1 mRNA+	GTGGAGAAAGGGGAGACCAT
NRDG1 mRNA-	ACAGCGTGACGTGAACAGAG

siRNA sequences

siAR1 (Dharmacon ON TARGET plus siRNA)	(1)GGAACUCGAUCGUAUCAUU (2)CAAGGGAGGUUACACCAAA (3)UCAAGGAACUCGAUCGUAU

	(4)GAAAUGAUUGCACUAUUGA
siAR2 (Haag et al., 2005)	GACCUACCGAGGAGCUUUC
siFoxA1 (Carroll et al., 2005)	GAGAGAAAAAAUCAACAGC
siGATA2 (Dharmacon ON TARGET plus siRNA)	(1)UCGAGGAGCUGUCAAAGUG
	(2)ACUACAAGCUGCACAAUGU
	(3)GAAGAGCCGGCACCUGUUG
	(4)GCCCAGGCCUAGCUACUAU
siUBE2C (Dharmacon ON TARGET plus siRNA)	(1)GAACCCAACAUUGAUAGUC
	(2)UAAAUUAAGCCUCGGUUGA
	(3)GUAUAGGACUCUUUAUCUU
	(4)GCAAGAAACCUACUCAAAG
siMED1 (Dharmacon siGenome siRNA)	(1)GCAGAGAAAUCUUAUCAGA
	(2)CCAUUAAGCUUGUGCGUCA
	(3)CAGCAAUGACUGAUCGUUU
	(4)GGCCGAAGAGCAAGGCUUA
siCDK1 (Dharmacon ON TARGET plus siRNA)	(1)GGUUAUAUCUCAUCUUUGA
	(2)UCGGGAAAUUUCUCUAUUA
	(3)GUAUAAGGGUAGACACAAA
	(4)CAAACGAAUUUCUGGCAAA
siCDC20 (Dharmacon ON TARGET plus siRNA)	(1)CGGAAGACCUGCCGUUACA
	(2)GGGCCGAACUCCUGGCAAA
	(3)GAUCAAAGAGGGCAACUAC
	(4)CAGAACAGACUGAAAGUAC

Table S2

RefSeq numbers	Gene_name	Gene_locus	MAX AR binding locus wi	M phase	Distance_to_TSS	LNcap MATsco	LNcap FDR(%	abl_MATscore	abl_FDR (%)	LNCaP ChIP validation Fold over input (-/+DHT)	abl ChIP validation Fold over input (-/+DHT)	expression inc	expression inde	RT-PCR validati Fold (LNCaP/ab
NM_080816	SIRPG	chr20:155779	N/A	No	N/A	N/A	N/A	N/A	N/A	N/A	N/A	4.58218506	4.483470042	N/A
NM_018556	isoform of NM_080816	chr20:155779	N/A	No	N/A	N/A	N/A	N/A	N/A	N/A	N/A	4.52696721	4.489912814	N/A
NM_016262	TUBE1	chr6:1124986	N/A	No	N/A	N/A	N/A	N/A	N/A	N/A	N/A	5.70672923	5.233071301	N/A
NM_001786	CDC2	chr10:622082	chr10:62160949-621616	Yes	-46917	6.32	0.85	9.96	0	2.74/5.11	4.53/9.89	8.21329203	8.967081753	0.49
NM_033379	isoform of NM_001786	chr10:622099	chr10:62160949-621616	Yes	-48592	6.32	0.85	9.96	0	2.74/5.11	4.53/9.89	8.43914772	9.142799508	0.49
NM_014865	CNAP1	chr12:647355	N/A	Yes	N/A	N/A	N/A	N/A	N/A	N/D	N/D	6.81039042	7.922802155	N/A
NM_206825	GNL3	chr3:5269497	chr3:52697623-5269837	No	3023	1.73	N/A	4.76	4.96	0.98/1.4	1.58/3.37	9.73841304	9.290786148	1.2
NM_206826	isoform of NM_206825	chr3:5269497	chr3:52697623-5269837	No	3023	1.73	N/A	4.76	4.96	0.98/1.4	1.58/3.37	9.73841304	9.290786148	1.2
NM_014366	isoform of NM_206825	chr3:5269497	chr3:52697623-5269837	No	3023	1.73	N/A	4.76	4.96	0.98/1.4	1.58/3.37	9.73841304	9.290786148	1.2
NM_057749	CCNE2	chr8:9596163	N/A	No	N/A	N/A	N/A	N/A	N/A	N/A	N/A	5.59369809	6.741646704	N/A
NM_057735	isoform of NM_057749	chr8:9596163	N/A	No	N/A	N/A	N/A	N/A	N/A	N/A	N/A	5.59369809	6.741646704	N/A
NM_001827	CKS2	chr9:9111593	N/A	No	N/A	N/A	N/A	N/A	N/A	N/A	N/A	9.17222984	10.15144742	N/A
NM_001790	CDC25C	chr5:1376488	N/A	Yes	N/A	N/A	N/A	N/A	N/A	N/A	N/A	4.94401231	6.170019916	N/A
NM_022809	isoform of NM_001790	chr5:1376488	N/A	Yes	N/A	N/A	N/A	N/A	N/A	N/A	N/A	5.02547018	6.539295202	N/A
NM_001255	CDC20	chr1:4359721	chr1:43586290-4358704	Yes	-10547	0.91	N/A	4.18	5.64	1.21/2.03	2.24/2.94	7.00808947	9.065187135	0.43
NM_004219	PTTG1	chr5:1597814	N/A	Yes	N/A	N/A	N/A	N/A	N/A	N/A	N/A	8.79030912	10.51114977	N/A
NM_003035	STIL	chr1:4748839	N/A	No	N/A	N/A	N/A	N/A	N/A	N/A	N/A	5.44311542	6.424333732	N/A
NM_006191	PA2G4	chr12:547843	N/A	No	N/A	N/A	N/A	N/A	N/A	N/A	N/A	7.8224597	6.829515049	N/A
NM_016359	NUSAP1	chr15:394123	N/A	Yes	N/A	N/A	N/A	N/A	N/A	N/A	N/A	7.51838671	9.227392953	N/A
NM_018454	isoform of NM_016359	chr15:394123	N/A	Yes	N/A	N/A	N/A	N/A	N/A	N/A	N/A	7.51838671	9.227392953	N/A
NM_152524	SGOL2	chr2:2010991	N/A	No	N/A	N/A	N/A	N/A	N/A	N/A	N/A	4.85860638	7.108055357	N/A
NM_012415	RAD54B	chr8:9545336	N/A	Yes	N/A	N/A	N/A	N/A	N/A	N/A	N/A	5.09715134	6.493933597	N/A
NM_007019	UBE2C	chr20:438746	chr20:43841021-4384177	Yes	-33265	1.69	N/A	5.35	0.48	1.14/2.67	2.73/7.55	7.95370942	9.4174472	0.43
NM_181803	isoform of NM_007019	chr20:438746	chr20:43841021-4384177	Yes	-33265	1.69	N/A	5.35	0.48	1.14/2.67	2.73/7.55	8.40600671	10.14054329	N/A
NM_181802	isoform of NM_007019	chr20:438746	chr20:43841021-4384177	Yes	-33265	1.69	N/A	5.35	0.48	1.14/2.67	2.73/7.55	7.95370942	9.4174472	0.43
NM_181800	isoform of NM_007019	chr20:438746	chr20:43841021-4384177	Yes	-33265	1.69	N/A	5.35	0.48	1.14/2.67	2.73/7.55	7.64577392	9.224184332	0.43
NM_181801	isoform of NM_007019	chr20:438750	chr20:43841021-4384177	Yes	-33664	1.69	N/A	5.35	0.48	1.14/2.67	2.73/7.55	7.95370942	9.4174472	0.43
NM_181799	isoform of NM_007019	chr20:438746	chr20:43841021-4384177	Yes	-33265	1.69	N/A	5.35	0.48	1.14/2.67	2.73/7.55	8.85002557	10.39395483	N/A
NM_002165	ID1	chr20:296567	chr20:29639157-296399	No	-17220	3.97	10.27	1.06	N/A	0.32/0.49	0.27/0.26	3.76052332	7.86913246	0.026
NM_181353	isoform of NM_002165	chr20:296567	chr20:29639157-296399	No	-17220	3.97	10.27	1.06	N/A	0.32/0.49	0.27/0.26	3.76052332	7.86913246	0.026
NM_078467	CDKN1A	chr6:3675446	chr6:36754833-3675558	No	744	8.03	0.33	3.95	11.43	4.55/10.75	1.55/4	8.95474486	8.483660584	1.08
NM_000389	isoform of NM_078467	chr6:3675446	chr6:36754833-3675558	No	744	8.03	0.33	3.95	11.43	4.55/10.75	1.55/4	8.95474486	8.483660584	N/A
NM_001007793	BUB3	chr10:124903	chr10:124890022-12489	Yes	-13462	3	N/A	5.25	1.32	3.22/5.84	5.19/8.42	9.11864956	9.094199591	0.85
NM_006806	BTG3	chr21:178878	chr21:17896368-1789711	No	10290	0.33	N/A	4.28	14.63	0.34/0.33	0.89/1.7	7.92146396	8.13885979	0.96
NM_016567	BCCIP	chr10:127502	chr10:127502735-12750	No	1006	2.96	N/A	5.37	0.92	1.48/3.13	3.1/7.55	7.70028236	7.658222404	1.15
NM_002198	IRF1	chr5:1318466	N/A	No	N/A	N/A	N/A	N/A	N/A	N/A	N/A	5.49159723	5.851208001	N/A
NM_018492	PBK	chr8:2772305	N/A	Yes	N/A	N/A	N/A	N/A	N/A	N/A	N/A	7.38932565	9.415107145	N/A
NM_005879	TRAIP	chr3:4984103	N/A	No	N/A	N/A	N/A	N/A	N/A	N/A	N/A	4.31808238	5.528833817	N/A
NM_005192	CDKN3	chr14:539334	chr14:53977126-5397787	No	44026	4.7	3.2	1.51	N/A	1.06/1.88	0.95/0.91	6.85142272	8.639640953	4.82
NM_144665	SESN3	chr11:945457	N/A	No	N/A	N/A	N/A	N/A	N/A	N/A	N/A	7.69789296	7.332408968	N/A
NM_006716	DBF4	chr7:8734347	chr7:87343219-8734396	No	115	4.36	5.3	1.32	N/A	6.72/8.43	1.61/2.35	4.25859625	5.97364262	0.33
NM_012406	PRDM4	chr12:106650	chr12:106677445-10667	No	1224	3.86	8.46	1.15	N/A	2.18/4.46	2.19/2.52	6.55035025	6.470557094	1.24
NM_014750	DLG7	chr14:546846	N/A	Yes	N/A	N/A	N/A	N/A	N/A	N/A	N/A	6.29524702	8.073699613	N/A
NM_002201	ISG20	chr15:869830	N/A	No	N/A	N/A	N/A	N/A	N/A	N/A	N/A	6.35851262	6.642775083	N/A
NM_018101	CDCA8	chr1:3793074	N/A	No	N/A	N/A	N/A	N/A	N/A	N/A	N/A	7.16916153	8.247358692	N/A
NM_004935	CDK5	chr7:1503818	N/A	No	N/A	N/A	N/A	N/A	N/A	N/A	N/A	8.29366812	7.840165371	N/A
NM_006101	KNTC2	chr18:256160	N/A	Yes	N/A	N/A	N/A	N/A	N/A	N/A	N/A	5.46444853	7.024865273	N/A
NM_001237	CCNA2	chr4:1229579	chr4:122962258-122963	Yes	1697	5.95	2.04	3.68	N/A	1.89/8.08	1.38/6.54	5.9705573	7.257637087	0.47
NM_198315	LOH11CR2A	chr11:123491	N/A	No	N/A	N/A	N/A	N/A	N/A	N/A	N/A	5.69398091	5.22172828	N/A
NM_005862	STAG1	chr3:1375386	N/A	Yes	N/A	N/A	N/A	N/A	N/A	N/A	N/A	5.35793355	5.624377654	N/A
NM_004365	CETN3	chr5:8972528	N/A	Yes	N/A	N/A	N/A	N/A	N/A	N/A	N/A	8.55036787	8.280063382	N/A
NM_014885	ANAPC10	chr4:1461357	chr4:146206463-1462072	Yes	31953	3.66	10.69	5.42	0.48	1.1/3.41	1.64/5.02	5.70063313	6.494122565	0.58

Supplemental Experimental Procedures

ChIP assays

Antibodies used were as follows: anti-AR (N20), anti-GATA2 (H116), anti-Oct1 (C21) and anti-MED1 (M255) from Santa Cruz Biotechnology (Santa Cruz, CA), anti-FoxA1 (ab23738), anti-H3K4me1 (ab8895), anti-H3K4me2 (ab7766) and anti-H3K4me3 (ab8580) from Abcam (Cambridge, MA).

Western blot analysis

Antibodies used were anti-AR (441), anti-CDK1 (17), anti-PSA (C19), anti-GATA2 (H116), anti-Oct1 (C21) and anti-MED1 (M255) from Santa Cruz Biotechnology, anti-CDC20 (ab26483) and anti-FoxA1 (ab23738) from Abcam, anti-UBE2C (A650) from Boston Biochem (Cambridge, MA), An antibody against KDM1 was a gift from Roland Schule (Universitäts-Frauenklinik und Zentrum für Klinische Forschung, Freiburg, Germany).

Quantitative chromosome conformation capture assay (3C-qPCR)

The data was normalized for primer efficiency difference using BAC RP11-75C3 that covers the UBE2C locus, and for DNA concentration difference using a GADPH loading control. In addition, the interaction of two Bgl II sites in the GADPH locus was used to correct for difference in crosslinking and digestion efficiencies between different cell lines as previously described (Duan et al., 2008; Hakim et al., 2009). The Taqman probe and primer sequences are listed in Table S1.

Tissue microarray analysis

The tissue microarray slides were scanned using the Ariol image analysis system (Applied Imaging Inc, San Jose, CA) at 20x objective magnification. Each specimen was represented by 2 to 3 tissue microarray cores. Each core of the tissue microarray was then marked so that only one specific tissue type is represented in each core. Using the MultiStain assay, an appropriate classifier was developed that can pick out the area of positive staining and count the number of nuclei that were positively stained. Additionally, the classifier was developed to count negative nuclei. Subsequently, the tissue microarrays were analyzed using this classifier and scores were calculated using the data given. The Nuclear Staining Score was given by the formula log10 (((Intensity Score)*(Percentage positive nuclei)) + 1) while the Total Staining Score was given by log10 (((Intensity Score)*(Percentage pixels positively stained) + 1).

Supplemental References

Bieche, I., Parfait, B., Tozlu, S., Lidereau, R., and Vidaud, M. (2001). Quantitation of androgen receptor gene expression in sporadic breast tumors by real-time RT-PCR: evidence that MYC is an AR-regulated gene. Carcinogenesis *22*, 1521-1526.

Carroll, J.S., Liu, X.S., Brodsky, A.S., Li, W., Meyer, C.A., Szary, A.J., Eeckhoute, J., Shao, W., Hestermann, E.V., Geistlinger, T.R., *et al.* (2005). Chromosome-wide mapping of estrogen receptor binding reveals long-range regulation requiring the forkhead protein FoxA1. Cell *122*, 33-43.

Duan, H., Xiang, H., Ma, L., and Boxer, L.M. (2008). Functional long-range interactions of the IgH 3' enhancers with the bcl-2 promoter region in t(14;18) lymphoma cells. Oncogene *27*, 6720-6728.

Haag, P., Bektic, J., Bartsch, G., Klocker, H., and Eder, I.E. (2005). Androgen receptor down regulation by small interference RNA induces cell growth inhibition in androgen sensitive as well as in androgen independent prostate cancer cells. J Steroid Biochem Mol Biol *96*, 251-258.

Hagege, H., Klous, P., Braem, C., Splinter, E., Dekker, J., Cathala, G., de Laat, W., and Forne, T. (2007). Quantitative analysis of chromosome conformation capture assays (3C-qPCR). Nat Protoc *2*, 1722-1733.

Hakim, O., John, S., Ling, J.Q., Biddie, S.C., Hoffman, A.R., and Hager, G.L. (2009). Glucocorticoid receptor activation of the ciz1-lcn2 locus by long range interactions. J Biol Chem *284*, 6048-6052.

Jia, L., Kim, J., Shen, H., Clark, P.E., Tilley, W.D., and Coetzee, G.A. (2003). Androgen receptor activity at the prostate specific antigen locus: steroidal and non-steroidal mechanisms. Mol Cancer Res *1*, 385-392.

Lofstedt, T., Jogi, A., Sigvardsson, M., Gradin, K., Poellinger, L., Pahlman, S., and Axelson, H. (2004). Induction of ID2 expression by hypoxia-inducible factor-1: a role in dedifferentiation of hypoxic neuroblastoma cells. J Biol Chem *279*, 39223-39231.

Okamoto, Y., Ozaki, T., Miyazaki, K., Aoyama, M., Miyazaki, M., and Nakagawara, A. (2003). UbcH10 is the cancer-related E2 ubiquitin-conjugating enzyme. Cancer Res *63*, 4167-4173.

Reddy, S.K., Rape, M., Margansky, W.A., and Kirschner, M.W. (2007). Ubiquitination by the anaphase-promoting complex drives spindle checkpoint inactivation. Nature *446*, 921-925.

Schuur, E.R., Henderson, G.A., Kmetec, L.A., Miller, J.D., Lamparski, H.G., and Henderson, D.R. (1996). Prostate-specific antigen expression is regulated by an upstream enhancer. J Biol Chem *271*, 7043-7051.

Sun, Z., Pan, J., and Balk, S.P. (1997). Androgen receptor-associated protein complex binds upstream of the androgen-responsive elements in the promoters of human prostate-specific antigen and kallikrein 2 genes. Nucleic Acids Res *25*, 3318-3325.

Wang, Q., Carroll, J.S., and Brown, M. (2005). Spatial and temporal recruitment of androgen receptor and its coactivators involves chromosomal looping and polymerase tracking. Mol Cell *19*, 631-642.

Wang, Q., Li, W., Liu, X.S., Carroll, J.S., Janne, O.A., Keeton, E.K., Chinnaiyan, A.M., Pienta, K.J., and Brown, M. (2007). A hierarchical network of transcription factors governs androgen receptor-dependent prostate cancer growth. Mol Cell *27*, 380-392.

Yu, D.C., Sakamoto, G.T., and Henderson, D.R. (1999). Identification of the transcriptional regulatory sequences of human kallikrein 2 and their use in the construction of calydon virus 764, an attenuated replication competent adenovirus for prostate cancer therapy. Cancer Res *59*, 1498-1504.

Yu, J., Rhodes, D.R., Tomlins, S.A., Cao, X., Chen, G., Mehra, R., Wang, X., Ghosh, D., Shah, R.B., Varambally, S., *et al.* (2007). A polycomb repression signature in metastatic prostate cancer predicts cancer outcome. Cancer Res *67*, 10657-10663.

Yuan, B., Xu, Y., Woo, J.H., Wang, Y., Bae, Y.K., Yoon, D.S., Wersto, R.P., Tully, E., Wilsbach, K., and Gabrielson, E. (2006). Increased expression of mitotic checkpoint genes in breast cancer cells with chromosomal instability. Clin Cancer Res *12*, 405-410.